E11-2009-174

P. Kopcansky[1], M. Timko[1], M. Hnatic[1,2,3], M. Vala[1,2,3],
G. M. Arzumanyan[3], E. A. Hayryan[3], L. Jancurova[3,4],
J. Jadlovsky[4], J. Chovanak[4]

THE CONCEPT OF FOCUSED MAGNET FOR TARGETED DRUG DELIVERY

[1]Institute of Experimental Physics, SAS, Kosice, Slovakia
[2]Faculty of Science, Pavol Jozef Safarik University, Kosice, Slovakia
[3]Joint Institute for Nuclear Research, Dubna
[4]Faculty of Electrical Engineering and Informatics, Technical University, Kosice, Slovakia

Копчански П. и др. E11-2009-174
Концепция сфокусированного магнита,
предназначенного для доставки лекарств

Сконструирован специальный сфокусированный магнит, служащий для доставки лекарственных средств в предназначенное место. Теоретические расчеты вместе с условием прилипания капли магнитной жидкости в магнитном поле показали, что такой магнит создает достаточное магнитное поле для прилипания магнитных частиц на стенке сосуда и может использоваться на 2,5–3 см глубже в организме по сравнению с призмовым постоянным магнитом, что позволяет бесконтактный перенос лекарства с помощью данного магнита. Максимальные значения магнитного поля и градиента магнитного поля составляют 0,38 Тл и 101 Тл/м.

Работа выполнена в Лаборатории информационных технологий ОИЯИ.

Сообщение Объединенного института ядерных исследований. Дубна, 2009

Kopcansky P. et al. E11-2009-174
The Concept of Focused Magnet for Targeted Drug Delivery

A special focused magnet, designed for the use in the magnetic targeted drug delivery system, was constructed. The theoretical calculation of the adhesion condition for a magnetic fluid drop in magnetic field with obtained design showed that the constructed focused magnet generates a sufficient magnetic force for the capture of a magnetic drop on the vessel wall and can be used 2.5–3 cm deeper in an organism compared with the prism permanent magnet which could enable the non-invasivity of the magnetic drug targeting procedure. The maximal values for the magnetic field and gradient of the magnetic field are 0.38 T and 101 T/m.

The investigation has been performed at the Laboratory of Information Technologies, JINR.

Communication of the Joint Institute for Nuclear Research. Dubna, 2009

The difference between success and failure of chemotherapy depends not only on the drug itself but also on how it is delivered to its target. One of the major problems in pharmacotherapy is the delivery of drugs to a specific location and maintenance of its location for the desired length of time. Because of the relatively non-specific action of chemotherapeutic agents, there is almost always some toxicity to normal tissues. Therefore, it is of great importance to be able to selectively target the magnetically labelled drug to the tumor target as precisely as possible, to reduce resulting systemic toxic side effects from generalized systemic distribution and to be able to use a much smaller dose, which would further lead to a reduction of toxicity. The method of magnetic drug targeting is dependent on physical properties, concentration and number of applied nanoparticles, on type of binding of the drugs, on the physiological parameters of the patient and of course on magnetic force, which is defined by its field and field gradient [1]. Guided transport of biologically active substances to the target organ allows creating an optimum therapeutic concentration of the drug in the desired part of organism, while keeping the total injected dose low [2–4]. Current research on methods to target chemotherapy drugs in the human body includes the investigation of biocompatible magnetic nano-carrier systems, e.g., magnetic liquids such as ferrofluids. The use of biocompatible magnetic fluid as potential drug carrier appears to be a promising technique. Due to their superparamagnetic properties the magnetic fluid drops can be precisely transported, positioned and controlled in desirable parts of blood vessels or hollow organs with the help of an external magnetic field. The motion of magnetic drop within the body is controlled by the combination of magnetic force and a hemodynamic drag force due to blood flow. The models which investigate the interaction of an external magnetic field with blood flow containing a magnetic carrier substance are based on the Maxwell and Navier–Stokes equations, where a static magnetic field is coupled to fluid flow. This is achieved by adding a magnetic volume force to the Navier–Stokes equations, which stems from the solution of magnetic field problem [5]. In order to effectively overcome the influence of blood flow the magnetic force must be larger than the drag force. The conditions for holding a magnetic fluid drop on a blood vessel wall were investigated by Voltairas et al. [6]. In this work the non-uniformity of considered magnetic field was higher only close to the magnetic pole, which was regarded as a major technical problem that has to be resolved in order for the drug targeting to remain essentially non-invasive. The aim of our work was to construct a focused magnet, which enables one to achieve

maximal magnetic force in deeper position, to map its magnetic field and to find the adhesion condition for a magnetic fluid drop in magnetic field with obtained design. Voltairas et al. [6] presented a self-consistent ferrohydrodynamic theory of magnetic drug targeting and examined a model case to account for adhesion. They obtained an upper bound of the mean blood flow velocity as a function of the applied magnetic field, which was considered to be produced by a point source located outside the body at $x = -\delta$, $y = 0$, $z = \zeta$ (δ, $\zeta > 0$ non-uniformity higher only close to magnetic pole) and had the form

$$\vec{H} = \frac{m(\vec{r} + \delta\hat{e}_x - \zeta\hat{e}_z)}{(r^2 + \delta^2 + \zeta^2 + 2\delta x - 2\zeta z)^{\frac{3}{2}}}, \tag{1}$$

where m is the magnetic dipole moment. The magnetic point source was oriented at an angle

$$\omega = \arcsin\left(\frac{\zeta}{\delta}\right) \tag{2}$$

with respect to the x axis. The found adhesion condition in dimensionless form reads

$$\frac{1}{B_m} = \frac{\chi}{4S_0} \iint\limits_{S_1} \left(h^2 + h_n^2\right) dS, \tag{3}$$

where

$$B_m = \frac{\mu_0 H_0^2 R}{\gamma} \tag{4}$$

is the magnetic bond number with R being the radius of the magnetic drop and

$$h = \frac{H}{H_0}, \quad h_n = \frac{H_n}{H_0}, \quad H_0 = \frac{m}{\delta^2}, \quad S_0 = 2\pi R^2 \tag{5}$$

with

$$H_n = \hat{n}H.$$

An additional global condition, taking into account the deformation of the magnetic drop due to the blood flow, was derived in the form

$$V_m = \frac{\chi}{2\beta S_0} \iint\limits_{S_0} \left[\left(h^2 - (1 + 2\chi)\, h_n^2\right) \hat{n}_z + 2\chi\,(1 + \chi)\, h_n h_z\right] dS, \tag{6}$$

where

$$V_m = \frac{\eta_2 u_0}{\mu_0 H_0^2 R} \tag{7}$$

is the dimensionless velocity and

$$\beta = \frac{\gamma_v - 1}{\gamma_v + 1}, \quad \gamma_v = \frac{\eta_2}{\eta_1}, \quad h_z = \frac{H_z}{H_0}. \tag{8}$$

Here η_2 is the blood viscosity, η_1 is the viscosity of magnetic fluid and u_0 is the mean blood flow velocity.

Thus, instead of one adhesion condition, Voltairas et al. [6] obtained two equations (9) and (10), and the dependence of blood flow velocity on the applied magnetic field was parameterized as

$$B_m = B_m(R,\, \delta,\, \chi,\, \omega) \tag{9}$$

and

$$V_m = V_m\left(R,\, \delta,\, \chi,\, \omega,\, \gamma_0\right). \tag{10}$$

The obtained law $V_m = V_m\left(B_m\right)$ gives an upper bound of the mean blood flow velocity, at which the applied magnetic field is able to capture a magnetic drug drop on the blood vessel wall. To achieve a proper non-uniform magnetic field, able to localize a magnetic drop inside the body, two types of magnets could be used — permanent magnets or electromagnets. The permanent magnets generate magnetic fields, which are rather weak for the trapping of magnetic drop in a bulk vessel. The electromagnets generate stronger magnetic fields; however, they need an outer source of electrical current and they produce the Joule heat. Our aim was to develop an arrangement of permanent magnets which could generate higher induction and gradient of magnetic field than classical magnets with simple geometry. The first step in the manufacturing of such a focused magnet was a theoretical optimization of magnetic field generated by a permanent magnet. Let us have a closed part of space called Ω, filled with permanent magnet or a frame of permanent magnets. The magnitude of the magnetization M is given by the properties of the used material. Our question is: At which orientation of the magnetization in Ω will the maximal projection of induction B into the direction s in point F (Fig. 1) be achieved?

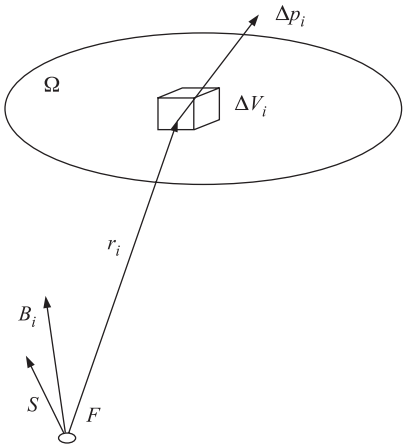

Fig. 1. The illustration of the studied problem: Ω — closed part of space filled with permanent magnet; B_i — magnetic induction generated by magnetic moment $\Delta p_i = M\left(r_i\right)\Delta V_i$

The volume Ω can be divided into the elements ΔV_i with position vectors $\mathbf{r}_i$ starting in point F. The magnetic induction B in point F is then the sum of contributions ΔB_i generated by magnetic moments $\Delta p_i = M\left(r_i\right)\Delta V_i$. The

radial, tangential and azimuthal components of contribution ΔB_i are

$$\Delta B_{i,r} = \frac{\Delta p_i}{r^3} 2 \cos\, \alpha_i, \tag{11}$$

$$\Delta B_{i,\Theta} = \frac{\Delta p_i}{r^3} \sin\,(-\alpha_i), \tag{12}$$

$$\Delta B_{i,\varphi} = 0, \tag{13}$$

respectively, where α_i is the angle between Δp_i and r_i. The projection $\Delta B_{i,s}$ of vector ΔB_i into the direction s is a sum of the projections of its components. The projection of radial component is $\Delta B_{i,r} \cos\, \upsilon_i$, where υ_i is the angle between the vectors s and r. The projection of tangential component at fixed α_i and υ_i is maximal, if the vectors s, Δp_i and r_i lie in the same plane and the azimuthal angle of vectors s and Δp_i, with respect to positional vector r_i, is equal to π. Then this projection is equal to $\Delta B_{i,\Theta} \sin\,(-\upsilon_i)$ and

$$\Delta B_{i,s} = \Delta B_{i,r} \cos\, \upsilon_i + \Delta B_{i,\Theta} \sin\,(-\upsilon_i)\,. \tag{14}$$

By using Eqs. (11) and (12), the projection $\Delta B_{i,s}$ can be expressed as

$$\Delta B_{i,s} = \frac{\Delta p_i}{r_i^3} \left(2 \cos\, \alpha_i \cos\, \upsilon_i + \sin\, \alpha_i \sin\, \upsilon_i\right). \tag{15}$$

The optimizing condition for $\Delta B_{i,s}$ reads

$$\frac{d\left(\Delta B_{i,s}\right)}{d\left(0\right)} = 0 \tag{16}$$

with fields

$$-2 \sin\, \alpha_i \cos\, \alpha_i + \cos\, \alpha_i \sin\, \alpha_i = 0. \tag{17}$$

Thus, the angle α_i is optimal if

$$\tan \alpha_i = \frac{1}{2} \tan \upsilon_i. \tag{18}$$

This condition determines the direction of the lines of force of magnetic field generated by a fictive dipole with direction s, located in point F. If condition Eq. (18) is accomplished in all volume elements of Ω, then the sum of their contributions will be also optimal. Now we can summarize: If the magnetization of permanent magnet (system of permanent magnets) parallel to lines of force of a dipole with direction s, localized in point F, then the projection of magnetic induction generated by this magnet into direction s in point F will be optimal. This theoretical background was consecutively used for suggestion design and

construction of special focused magnet. The principle of magnetic focusing, consisting in the fulfilment of condition Eq. (18), is presented in Fig. 2 for the simple case of prism.

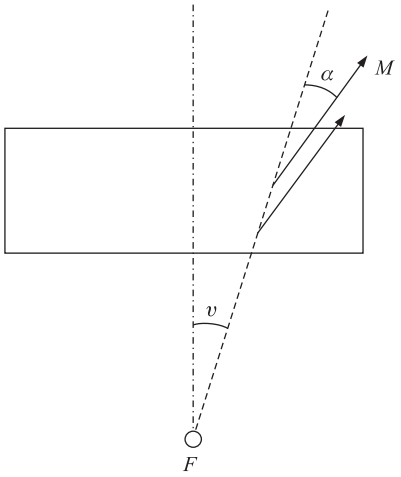

Fig. 2. The magnetic focusing corresponding to the condition $\tan\alpha_i = \frac{1}{2}\tan\nu_i$

It is evident that manufacturing such a magnet from one piece would be very problematic. Nevertheless, some approach which realizes the principle at least in reasonable approximation should be viable. We could apply the information that the direction of magnetization is parallel to the straight lines passing the focus (see Fig. 2). It means that the magnet could be composed of pyramids with peaks in focus F; the direction of the magnetization in the pyramids should be parallel — satisfying approximately the condition given by Eq. (18). Following the above-mentioned considerations and taking into account the technological simplicity, we proposed the construction of compound focused magnet. Its cross section is schematically drawn in Fig. 3.

Using a computer model, in which magnetic field and its gradient for different focus distances were calculated, the parameters of the focused magnet were compared with a prism magnet. The found results are presented in Figs. 4 and 5.

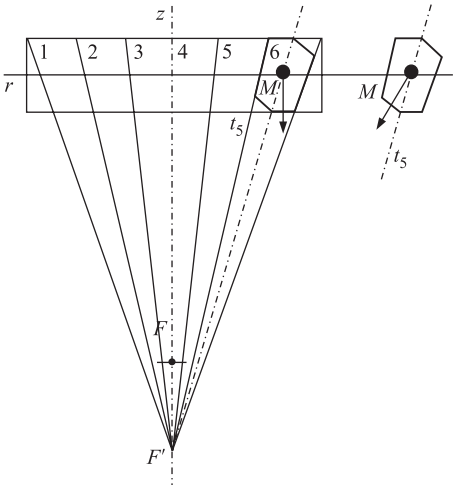

Fig. 3. The cross section of the focused magnet

The original FeNdB magnet had a form of rectangular prism ($40\times40\times10$ mm), the preferred direction of magnetization was perpendicular to its greatest side. Before the magnetization the magnet was cut into six prisms by an electro-spark cutter, according to the scheme shown in Fig. 3. Moreover, each prism was shaped in such a way that its cross section became symmetric about the axis crossing its center of mass and peak F'. This modification is shown for prism No. 6. Then the prisms were turned through 180° around the axes t_i;

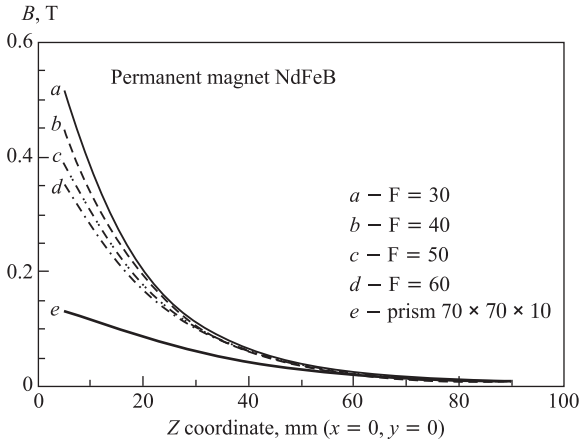

Fig. 4. The magnetic field calculated for the proposed focused magnet, comparison with prism magnet (F — focus distance of the proposed magnet in mm)

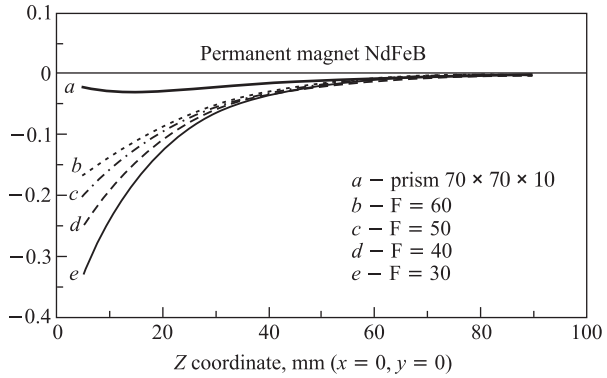

Fig. 5. The magnetic field gradient calculated for the proposed focused magnet, comparison with prism magnet

$i = 1$–6 and glued to their neighbours. The position of prism No. 6 after the gluing is shown on the right margin of Fig. 3 — it occupies the same part of space but the direction of the magnetization was changed as a consequence of rotation. After the gluing the cutting procedure to six prisms followed, according to the same scheme. The only difference was that the glued magnet was turned by right angle around the axis z before the new cutting, thus a checked structure of the magnet was obtained. The turning and gluing of the prisms was repeated and finally the compound intermediate magnet was obtained, with magnetization of each part directed into approximately one point on the axis z.

This point lies in the middle of the distance between the plane τ and peak F' (in plane τ the centers of mass of the parts of compound magnet lie). We remark that point F lies approximately in 3/4 of the distance τ–F'. After the second gluing the intermediate magnets were enclosed into a brass mantle and magnetized in a homogeneous magnetic field of 15 T. In this way the focused magnet, designed for the magnetic targeted drug delivery, was obtained.

The measured magnetic field by Hall probe was used for the construction of map of magnetic field of focused magnet. The examples of all componets of magnetic field, i.e., $B_x(x,\, y,\, z)$, $B_y(x,\, y,\, z)$, $B_z(x,\, y,\, z)$ are illustrated in Figs. 6–8 (for $y = 0.0$). As an example the function used for fitting of magnetic field $B_x(x,\, y,\, z)$ is given in Appendix.

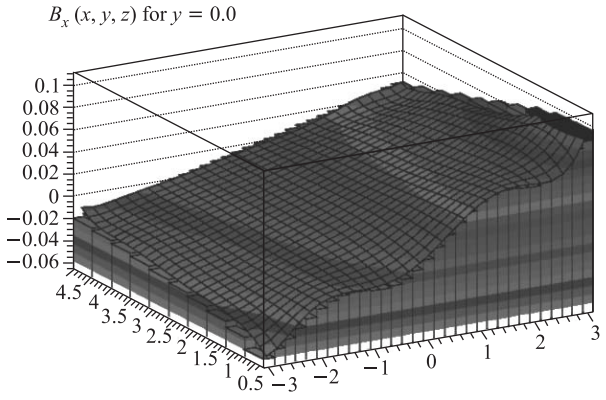

Fig. 6. The x component of magnetic field as a function of x, z for $y = 0.0$

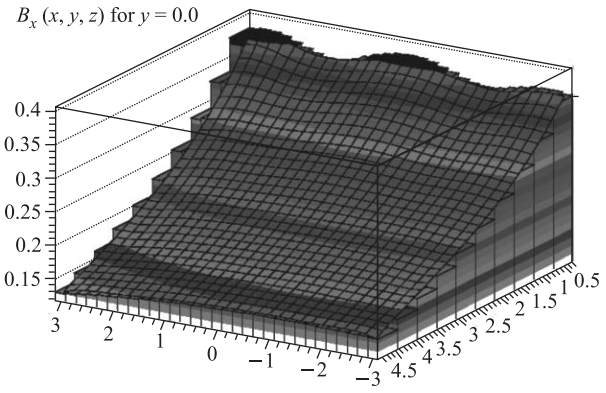

Fig. 7. The y component of magnetic field as a function of x, z for $y = 0.0$

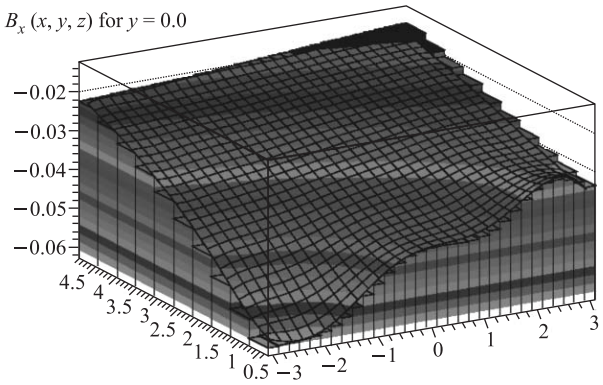

Fig. 8. The z component of magnetic field as a function of x, z for $y = 0.0$

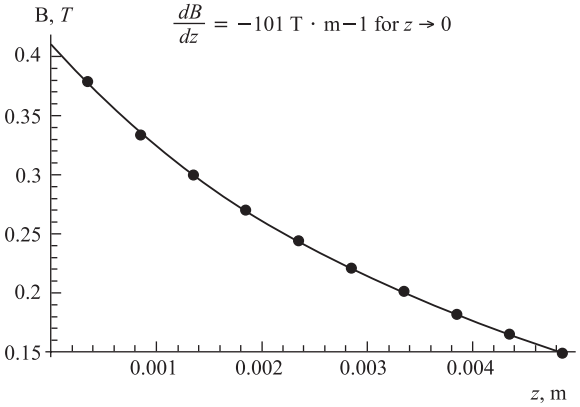

Fig. 9. The dependence of magnetic field induction generated by the manufactured focused magnet on the distance from the magnet surface and magnetic field gradient at $z = 0$

The maximal value of magnetic field near the magnet surface (0.35 mm) was estimated to be 0.38 T. The dependence of calculated values of the magnetic field gradient on the distance from the magnet surface in the axis z is given in Fig. 9.

For example, the magnetic field gradient at $z = 0$ was estimated to be 101 T/m. In an effort to test the ability of the magnet to generate a strong magnetic field in deeper position, the found profile of its magnetic field was used in the numerical calculation following the Voltairas et al. [6] model. The aim was to find the parameters for which the dependence B_m vs. V_m fits the curves obtained in [6]. The best fit, obtained for the distance between the pole of the magnet and the vessel wall 2.5–3 cm longer than that concerned in [6], is presented in Fig. 10.

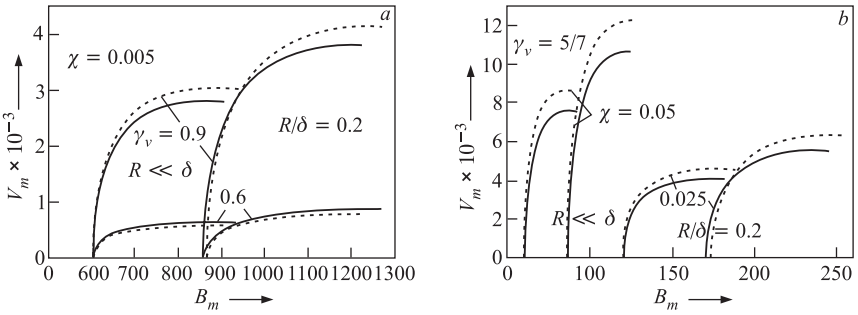

Fig. 10. The magnetic bond number B_m vs. V_m for $\chi = 0.005$ and varying γ_ν (*a*), and for $\gamma_\nu = 0.05$ and varying χ (*b*), both for $R/\delta = 0$ and $R/\delta = 0.2$ (dashed curves — results obtained by Voltairas et al.; solid curves — our fit)

So it can be said that using our specially focused magnet, a higher magnetic field, as well as its gradient, can be achieved in deeper position, which could enable the non-invasivity of the magnetic drug targeting procedure.

In summary, a focused magnet consisting of 36 prisms with pyramidal shape was manufactured, generating higher magnetic field and higher magnetic field gradient as compared with classical prism. The magnetic field of the focused magnet was mapped and its profile was used in numerical calculations, which yielded the upper bound of the mean blood flow velocity, at which the applied magnetic field is able to capture a magnetic drug drop on the blood vessel wall. The obtained results verified the ability of the magnet to generate a sufficient magnetic force in deeper position (2.5–3 cm), which could contribute to the non-invasivity of the magnetic drug targeting procedure.

Acknowledgements. This work was supported by the Project of Structural Funds of EU-Centrum Excellence: Cooperative Phenomena and Phase Transitions in Nanosystem with perspective utilization in Technics and Biomedicine No. 26220120021 and Centre of Excellence of Power Electronics Systems and Materials for Their Components No. 26220120003 which is funded by the European Community, ERDF — European Regional Development Fund and JINR Dubna protocol No. 33920-06-09/10 and the Russian Foundation of Basic Research Grants No. 08-01-00800-a and No. 07-01-00738-a.

REFERENCES

1. *Neuberger T., Schöpf B., Hofmann H., Hofmann M., Rechenberg B.* // J. Magn. Magn. Mater. 2005. V. 293. P. 483.
2. *Kuznetsov A. A., Filipov V. I., Kuznetsov O. A., Gerlivanov V. G., Dobrinsky E. K., Malashin S.I.* // J. Magn. Magn. Mater. 1999. V. 194. P. 22.
3. *Ruuge E. K., Rusetski A. N.* // J. Magn. Magn. Mater. 1993. V. 122. P. 335.

4. *Häfeli U. O., Pauer J. G.* // J. Magn. Magn. Mater. 1999. V. 194. P. 76.
5. *Ganguly R., Gaind A. P., Sen S., Puri I. K.* // J. Magn. Magn. Mater. 2005. V. 289. P. 331.
6. *Voltairas P. A., Fotiadis D. I., Michalis L. K.* // J. Biomech. 2002. V. 35. P. 813.

APPENDIX

$$F_x(x,\,y,\,z) = c_0 + c_1x + c_2y + c_3z + c_4x^2 + c_5y^2 + c_6z^2 + c_7xy + c_8yz + c_9zx + c_{10}x^3 + c_{11}y^3 + c_{12}z^3 + c_{13}x^2y + c_{14}xy^2 + c_{15}y^2z + c_{16}xz^2 + c_{17}z^2x + c_{18}zx^2 + c_{19}xyz + c_{20}x^4 + c_{21}y^4 + c_{22}z^4 + c_{23}x^3y + c_{24}x^3z + c_{25}y^3z + c_{26}y^3z + c_{27}z^3y + c_{28}z^3x + c_{29}x^2y^2 + c_{30}y^2z^2 + c_{31}z^2x^2 + c_{32}x^2yz + c_{33}y^2xz + c_{34}z^2xy + c_{35}x^5 + c_{36}y^5 + c_{37}z^5 + c_{38}x^4y + c_{39}x^4z + c_{40}y^4z + c_{41}y^4x + c_{42}z^4y + c_{43}z^4x + c_{44}x^3y^2 + c_{45}x^2y^3 + c_{46}y^3z^2 + c_{47}y^2z^3 + c_{48}z^3x^2 + c_{49}z^2x^3 + c_{50}x^3yz + c_{51}y^3xz + c_{52}z^3xy + c_{53}x^2y^2z + c_{54}x^2yz^2 + c_{55}y^2z^2x + c_{56}x^6 + c_{57}y^6 + c_{58}z^6 + c_{59}x^5y + c_{60}x^5z + c_{61}y^5z + c_{62}y^5x + c_{63}z^5y + c_{64}z^5x + c_{65}x^4y^2 + c_{66}x^2y^4 + c_{67}y^4z^2 + c_{68}y^2z^4 + c_{69}z^4x^2 + c_{70}z^2x^4 + c_{71}x^3y^3 + c_{72}x^3z^3 + c_{73}y^3z^3 + c_{74}x^4yz + c_{75}y^4xz + c_{76}z^4xy + c_{77}x^3y^2z + c_{78}x^3yz^2 + c_{79}y^3z^2x + c_{80}y^3zx^2 + c_{81}z^3x^2y + c_{82}z^3xy^2 + c_{83}x^2y^2z^2 + c_{84}x^7 + c_{85}y^7 + c_{86}z^7 + c_{87}x^6y + c_{88}x^6z + c_{89}x^4y^3 + c_{90}x^4z^3 + c_{91}x^3y^4 + c_{92}x^3z^4 + c_{93}x^2y^5 + c_{94}x^2z^5 + c_{95}xy^6 + c_{96}xz^6 + c_{97}x^5y^2 + c_{98}x^5z^2 + c_{99}y^6z + c_{100}y^5z^2 + c_{101}y^4z^3 + c_{102}y^3z^4 + c_{103}y^2z^5 + c_{104}yz^6 + c_{105}x^5yz + c_{106}x^4y^2z + c_{107}x^4yz^2 + c_{108}x^3y^3z + c_{109}x^3yz^3 + c_{110}x^3y^2z^2 + c_{111}x^2y^4z + c_{112}x^2yz^4 + c_{113}x^2y^3z^2 + c_{114}x^2y^2z^3 + c_{115}xy^5z + c_{116}xy^4z^2 + c_{117}xy^3z^3 + c_{118}xy^2z^4 + c_{119}xyz^5 + c_{120}x^8 + c_{121}y^8 + c_{122}z^8 + c_{123}x^7y + c_{124}x^7z + c_{125}x^6y^2 + c_{126}x^6z^2 + c_{127}x^5y^3 + c_{128}x^5z^3 + c_{129}x^4y^4 + c_{130}x^4z^4 + c_{131}x^3y^5 + c_{132}x^3z^5 + c_{133}x^2y^6 + c_{134}x^2z^6 + c_{135}y^7z + c_{136}y^6z^2 + c_{137}y^5z^3 + c_{138}y^4z^4 + c_{139}y^3z^5 + c_{140}y^2z^6 + c_{141}yz^7 + c_{142}xy^7 + c_{143}xz^7 + c_{144}x^6yz + c_{145}x^5y^2z + c_{146}x^5yz^2 + c_{147}x^4y^3z + c_{148}x^4y^2z^2 + c_{149}x^4yz^3 + c_{150}x^3y^4z + c_{151}x^3y^3z^2 + c_{152}x^3y^2z^3 + c_{153}x^3yz^4 + c_{154}x^2y^5z + c_{155}x^2y^4z^2 + c_{156}x^2y^3z^3 + c_{157}x^2y^2z^4 + c_{158}x^2yz^5 + c_{159}xy^6z + c_{160}xy^5z^2 + c_{161}xy^4z^3 + c_{162}xy^3z^4 + c_{163}xy^2z^5 + c_{164}xyz^6 + c_{165}x^9 + c_{166}y^5 + c_{167}z^5 + c_{168}x^8y + c_{169}x^8z + c_{170}x^7y^2 + c_{171}x^7z^2 + c_{172}x^6y^3 + c_{173}x^6z^3 + c_{174}x^5y^4 + c_{175}x^5z^5 + c_{176}x^4y^5 + c_{177}x^4z^5 + c_{178}x^3y^6 + c_{179}x^3z^6 + c_{180}x^2y^7 + c_{181}x^2z^7 + c_{182}xy^8 + c_{183}xz^8 + c_{184}y^8z + c_{185}y^7z^2 + c_{186}y^6z^3 + c_{187}y^5z^4 + c_{188}y^4z^5 + c_{189}y^3z^6 + c_{190}y^2z^7 + c_{191}yz^8 + c_{192}x^6y^2z + c_{193}x^6yz^2 + c_{194}x^5y^3z + c_{195}x^5y^2z^2 + c_{196}x^5yz^3 + c_{197}x^4y^4z + c_{198}x^7yz + c_{199}x^4y^3z^2 + c_{200}x^4y^2z^3 + c_{201}x^4y^1z^4 + c_{202}x^3y^5z + c_{203}x^3y^4z^2 + c_{204}x^3y^3z^3 + c_{205}x^3y^2z^4 + c_{206}x^3yz^5 + c_{207}x^2y^6z + c_{208}x^2y^5z^2 + c_{209}x^2y^4z^3 + c_{210}x^2y^3z^4 + c_{211}x^2y^2z^5 + c_{212}x^2yz^6 + c_{213}xy^7z + c_{214}xy^6z^2 + c_{215}xy^5z^3 + c_{216}xy^4z^4 + c_{217}xy^3z^5 + c_{218}xy^2z^6 + c_{219}xyz^7$$

Received on November 16, 2009.

Редактор *Е. И. Кравченко*

Подписано в печать 30.11.2009.
Формат 60 × 90/16. Бумага офсетная. Печать офсетная.
Усл. печ. л. 0,81. Уч.-изд. л. 1,13. Тираж 315 экз. Заказ № 56798.

Издательский отдел Объединенного института ядерных исследований
141980, г. Дубна, Московская обл., ул. Жолио-Кюри, 6.
E-mail: publish@jinr.ru
www.jinr.ru/publish/